Chronology, causes and progression of the Messinian salinity crisis

W. Krijgsman*, F. J. Hilgen†, I. Raffi‡, F. J. Sierro§ & D. S. Wilson‖

** Paleomagnetic Laboratory "Fort Hoofddijk", Utrecht University, Budapestlaan 17, 3584 CD Utrecht, The Netherlands*
† Department of Geology, Utrecht University, Budapestlaan 4, 3584 CD Utrecht, The Netherlands
‡ Dipartimento di Scienze della Terra, Università "G. D'Annunzio", Campus Universitario, Via dei Vestini 31, 66013 Chieti Scalo, Italy
§ Department de Geologia, Facultad de Ciencias, Universidad de Salamanca, 37008 93106, Salamanca, Spain
‖ Department of Geological Sciences, University of California, Santa Barbara, California 93106, USA

The Messinian salinity crisis is widely regarded as one of the most dramatic episodes of oceanic change of the past 20 or so million years (refs 1–3). Earliest explanations were that extremely thick evaporites were deposited in a deep and desiccated Mediterranean basin that had been repeatedly isolated from the Atlantic Ocean[1,2], but elucidation of the causes of the isolation—whether driven largely by glacio-eustatic or tectonic processes—have been hampered by the absence of an accurate time frame. Here we present an astronomically calibrated chronology for the Mediterranean Messinian age based on an integrated high-resolution stratigraphy and 'tuning' of sedimentary cycle patterns to variations in the Earth's orbital parameters. We show that the onset of the Messinian salinity crisis is synchronous over the entire Mediterranean basin, dated at 5.96 ± 0.02 million years ago. Isolation from the Atlantic Ocean was established between 5.59 and 5.33 million years ago, causing a large fall in Mediterranean water level followed by erosion (5.59–5.50 million years ago) and deposition (5.50–5.33 million years ago) of non-marine sediments in a large 'Lago Mare' (Lake Sea) basin. Cyclic evaporite deposition is almost entirely related to circum-Mediterranean climate changes driven by changes in the Earth's precession, and not to obliquity-induced glacio-eustatic sea-level changes. We argue in favour of a dominantly tectonic origin for the Messinian salinity crisis, although its exact timing may well have been controlled by the ~400-kyr component of the Earth's eccentricity cycle.

Most hypotheses about the initiation of the Messinian salinity crisis (MSC) agree that it resulted from a complex combination of tectonic and glacio-eustatic processes which progressively restricted and finally isolated the Mediterranean Sea from the open ocean[1–8]. The gradual modification of water exchange with the Atlantic caused important palaeoceanographic changes in the Mediterranean. This is reflected in the classic Messinian sequence of Sicily[9] which starts at 7.24 Myr ago (ref. 3) with alternations of open marine marls and sapropels, passes via diatomites into the Lower Evaporites (gypsum, evaporitic limestone and halite), and ends, above an erosional surface, with the Upper Evaporites (gypsum, marls) and fresh to brackish water deposits of Lago Mare facies. Here we define the MSC as the interval of evaporite deposition and Lago Mare sedimentation in the Mediterranean before the Pliocene flooding 5.33 Myr ago[10].

Controversies still exist, however, over the timing and duration of the MSC; these range from a synchronous event[1] (that is, onset of the MSC in all basins at the same time) to a two-step event[4] (onset of MSC first in marginal basins and later in deep basins) to a completely diachronous evolution[5] (onset of MSC totally dependent on local basinal setting). Equally large controversies exist over the cause, and the effects, of the isolation of the Mediterranean; the two basic explanations are (1) a large glacio-eustatic sea-level drop, related to expanding polar ice volume[6], and (2) orogenic uplift accompanied by gravity-driven sliding of large nappe complexes in the Gibraltar arc[7]. Until now, correlations of stable-isotope ($\delta^{18}O$ and $\delta^{13}C$) records from open-ocean sequences to the Messinian event stratigraphy of the Mediterranean have been ambiguous because of the absence of a reliable time frame for the MSC. The establishment of astronomical polarity timescales for the past 10 Myr (refs 3, 11) provided a significant advance in dating the geological record and promised a solution for the MSC controversies. Unfortunately, the Mediterranean-based astronomical polarity timescale showed a gap during much of the Messinian (6.7–5.3 Myr ago)[3], related to the presence of less-favourable sediments and the notoriously complex geological history of the Mediterranean in this time interval. However, the classic Messinian sediments display distinct sedimentary cyclicities, holding great promise for astronomical dating. Cyclostratigraphic and detailed palaeoclimatic studies revealed that the sedimentary cycles of the pre-evaporites are dominantly controlled by precession-induced changes in circum-Mediterranean climate[3,12,13].

To obtain a high-resolution cyclostratigraphic framework for the Messinian, we subjected three continuous pre-evaporite sequences of the western (Sorbas basin of Spain), central (Caltanissetta basin of Sicily) and eastern (Gavdos basin of Greece) Mediterranean to a detailed integrated stratigraphic study. All our stratigraphic records start at the Tortonian/Messinian boundary, and extend into the evaporites or evaporitic limestones of the MSC. Cyclostratigraphic correlations between the sections are straightforward, and have been confirmed by high-resolution biostratigraphy (Fig. 1). New magnetostratigraphic results were obtained from the Sorbas basin.

The starting point of our astronomical calibration is the previously established 'tuning' of early Messinian (up to 6.7 Myr ago) sequences[3]. Upward tuning, by calibrating younger cycles to successive insolation peaks[14], generally shows a good to excellent fit between the characteristic sedimentary cycle patterns and the astronomical target curve (Fig. 1), in particular the precession/obliquity interference patterns in the insolation curve. Alternating thick/thin beds consistently correlate with high/low amplitude variations in insolation, proving that no sedimentary cycles are missing and that alternative correlations can be ruled out. Nevertheless, some minor misfits can also be observed, which are probably due to small inaccuracies in the applied astronomical solution. Continuing research directed at improving the accuracy of the astronomical solution may result in minor modifications in the future, but this would not seriously affect the tuning and, hence, the Messinian astrochronology.

The two normal polarity intervals in the Sorbas magnetostratigraphy undoubtedly correspond to chrons C3An.1n and C3An.2n, respectively. Most recent timescales have dealt with poor age-control in the Messinian by recalibrating the marine magnetic anomaly ages for C3An (from Cande and Kent[15]) to match an age of ~5.23 Myr for the oldest Pliocene reversal[3,16]. Our astronomically tuned ages for the palaeomagnetic reversals of C3An, which are significantly older than in previous timescales (Table 1), close an important gap in the astronomical calibration.

Our magnetostratigraphy is confirmed by the position of the sinistral/dextral coiling change of *Neogloboquadrina acostaensis* in the middle of chron C3An.1r, in agreement with results from DSDP Site 609[17] of the adjacent Atlantic. Confirmation of our ages comes from open-ocean calcareous nannofossil biochronology. ODP Site 853 in the equatorial Pacific[18] has a reliable nannofossil biostratigraphy and magnetostratigraphy, but lacks a reliable astronomical tuning for the Miocene. ODP Site 926 in the equatorial Atlantic has reliable nannofossil events[19] and a straightforward astronomical tuning[20], but lacks a magnetostratigraphy. Assuming a low-latitude global synchroneity of the nannofossil events and exporting their

astronomical ages to the Pacific site allows us to calculate the ages of the palaeomagnetic reversals of C3An. These ages are in agreement with our ages (Table 1), indicating that both astronomical timescales are consistent with one another and confirming our age model for the Mediterranean Messinian. The age of the C3An.1n(y) reversal is especially well constrained because the 6.02-Myr LCO *Amaurolithus amplificus* datum occurs at 38.55–38.45 m in Hole 835B, indistinguishable from the 38.45-m depth of the reversal (Table 1). (Here LCO indicates last common occurrence.)

Support for our older ages for chron C3An is available from their implications for rates of sea-floor spreading. Detailed measurements of distances of tectonic-plate motion based on marine magnetic anomalies have provided a powerful test of the calibration of the Plio-Pleistocene reversal chronology[21], as spreading rates are often constant for intervals of 4 Myr or longer. Significant tectonic changes complicate the interpretation of the latest Miocene, but our revised ages provide the simplest picture of these changes (Fig. 2). Our timescale implies a constant rate of motion for Australia relative to Antarctica since 7 Myr ago, with a change then from 64 mm yr^{-1} to 69 mm yr^{-1} for a flowline at 98° E. Changes for Pacific Ocean plates are more dramatic, and because rates on different plate pairs change by different ratios, no possible timescale can yield constant rates for all plate pairs. Our ages yield the satisfying result that the largest rate change for each Pacific plate pair occurred simultaneously for all pairs at approximately 5.9 Myr. Previous age estimates[16] implied more complicated tectonic histories, generally

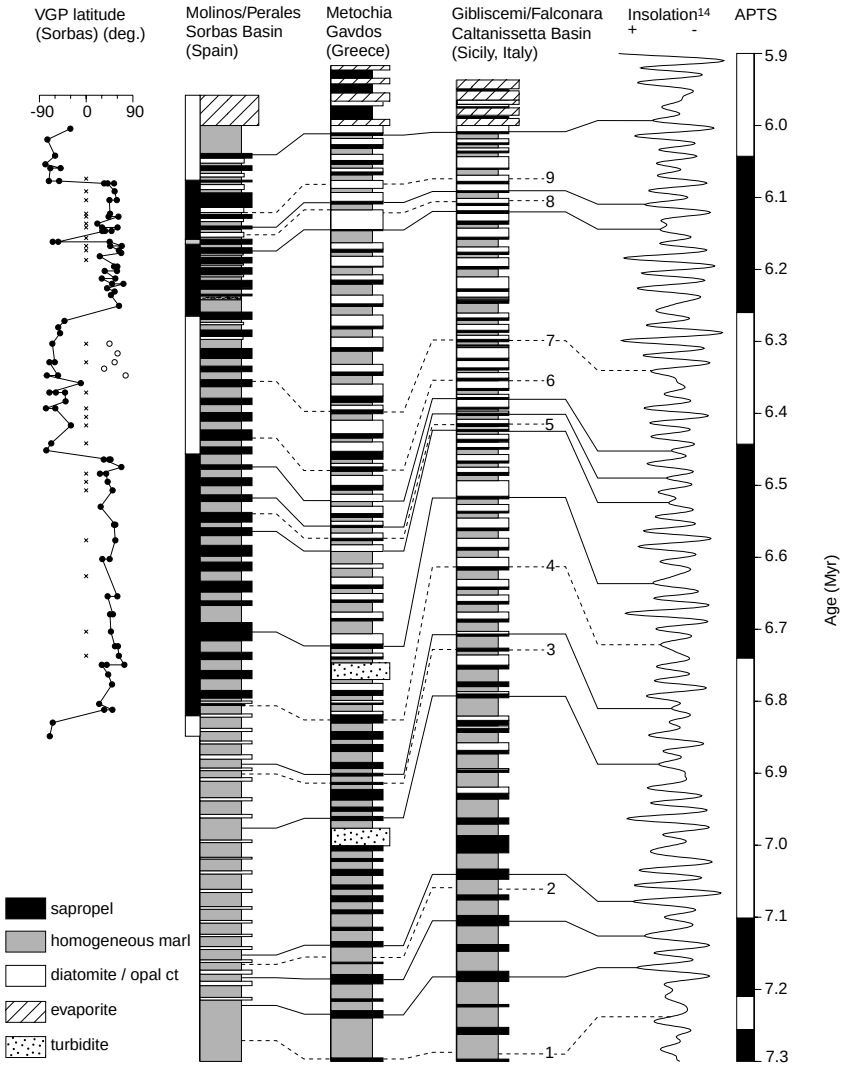

Figure 1 Astronomical calibration of Messinian pre-evaporite sequences. We used the La90 solution[14] with present-day (1,1) values for the dynamical ellipticity of the Earth and the tidal dissipation by the Moon as target curve, because it is the most accurate solution from a geological point of view[10]. Total thickness of the pre-evaporite section in Sorbas is 125 m, on Gavdos 31 m, and on Sicily 50 m. Sedimentary cyclicity in the Sorbas basin is characterized by an alternation of homogeneous marls and opal ct-rich beds in the lower part and of sapropels and homogeneous marls with irregularly intercalated diatomites in the upper part. Cyclicity on Gavdos and Sicily is bipartite (sapropel/marls) in the lower part and mainly tripartite (sapropel/diatomite/marl) in the upper part. Laminites (sapropels and diatomites) correspond to insolation maxima, homogeneous marls to insolation minima, with the exception of the lower part of Sorbas[13]. Magnetostratigraphic data from Sorbas are represented as virtual geomagnetic pole (VGP) latitude. Filled symbols denote samples with a palaeomagnetic signal sufficiently strong (0.01–0.1 mA m^{-1}) to determine the polarity. Open symbols denote directions interpreted as secondary overprint, crosses denote unreliable results. Cyclostratigraphic correlations are confirmed in detail by high-resolution planktonic foraminiferal biostratigraphy. Nine Mediterranean-wide planktonic foraminiferal bioevents are recognised: 1, first regular occurrence (FRO) of *Globorotalia conomiozea* group; 2, last occurrence (LO) of dominantly sinistral *Globorotalia scitula*; 3, *Globorotalia nicolae* FO; 4, *G. nicolae* LO; 5, *G. conomiozea* group LO; 6, first common occurrence (FCO) of *Turborotalita multiloba*; 7, sinistral/dextral coiling change *Neogloboquadrina acostaensis*; 8, first influx sinistral neogloboquadrinids (90%); 8, second influx sinistral neogloboquadrinids (40%). APTS (astronomical polarity timescale) is based on Sorbas data supplemented by earlier results from Crete[3].

involving faster apparent rates (more positive slopes) near 5.5 Myr ago and slower apparent rates near 7–8 Myr ago, as if the age of C3A is artificially young. Simultaneous rate changes by varying amounts on different Pacific plate pairs could easily be a consequence of a significant change in the absolute motion of the Pacific plate, as has been suggested by numerous authors for this time interval; for example, Cox and Engebretson[22]. Two studies have independently determined ages of 5.8–5.9 Myr (relative to C3An.1n(y) at 5.94–5.95 Myr) for a clockwise shift in motion direction of the Pacific plate relative to the Juan de Fuca plate[23] and the Antarctic plate[24]. According to the ages we determine here, the times of rate changes and direction changes are indistinguishable. As earlier shown for the Pliocene[21], it is evident that the astronomical polarity timescale for the late Miocene results in a more realistic spreading-rate history

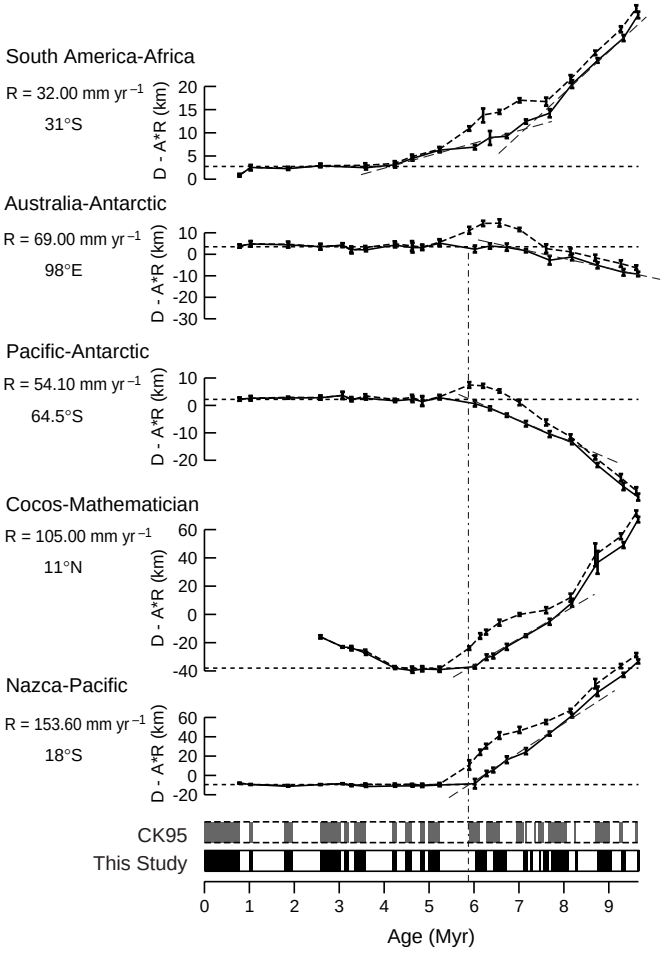

Figure 2 Late Neogene sea-floor spreading-rate histories. Reduced spreading distance versus age is shown for five plate pairs with intermediate-to-fast spreading rate and good data coverage. Reduced distance is simply the observed distance minus the predicted distance for a constant spreading rate. Distance scales are plotted inversely to the spreading rates so that, for plate pairs spreading constantly at the reduction rate, timescale errors will plot as uniform vertical departures from the reduction line. Our revised ages (solid lines) imply constant Australia–Antarctic and South America–Africa motion for 4–7 Myr and simultaneous changes on Pacific ocean plate pairs at 5.9 Myr (vertical line). All distance measurements are based on new determinations of rotation poles using digital data from the NGDC archive and miscellaneous recent cruises. Error bars are 95% confidence intervals for distance. Cocos–Mathematician data are from north of the Clipperton fracture zone, 10–13° N only; Pacific–Antarctic data are restricted to new data from 63–66° S[24]; Australia–Antarctic data from 94–138° E, Nazca–Pacific data from 1° N–30° S, and South America–Africa data from 25–29° S compiled by C. Weiland[32] span the well mapped and demonstrably rigid areas of the plates. *D*, distance; *A*, age; *R*, rate.

than does the most widely used geomagnetic polarity timescale (GPTS) of Cande and Kent[16].

The Messinian astrochonology that we report here solves many of the existing controversies over the MSC. The cyclostratigraphic results show that the transition to evaporite deposition (Lower Evaporites) occurs at the same sedimentary cycle in all sections. This proves that the MSC is a perfectly synchronous event over the entire Mediterranean, the onset of which is dated astronomically at 5.96 ± 0.02 Myr ago while the total duration is approximately 640 kyr. Deposition of the Lower Evaporite unit is thus independent of the palaeogeographic and geodynamic setting of the individual basins. The Lower Evaporites of Sorbas and Caltanissetta both require a continuously marine environment, excluding a relative sea-level fall exceeding the palaeodepth of these basins (that is, <200 m; ref. 25). This favours a deep-water model instead of a shallow-water (repetitive process of desiccating and reflooding) model for the deep (>1,000 m) Mediterranean basins. Complete isolation and possible desiccation was only established after deposition of the Lower Evaporites, when the Mediterranean water level dropped more than 1,000 m as shown by incised canyons of the Rhone, Ebro, Po and Nile rivers in the Mediterranean margins[4]. Deposition of the Upper Evaporite unit, overlying erosional surfaces, took place in a non-marine, deep Mediterranean basin forming a large Lago Mare[26]. Canyon incision in the Aegean region may have caused the transition to Lago Mare conditions by capturing the Black Sea drainage[1,26].

Our astronomically calibrated timescale for the Messinian now allows us to relate global environmental signals to the Mediterranean events. The most prominent (±50 m) glacio-eustatic sea-level falls (at oxygen isotope stages TG22 and TG20[27]), which are often suggested to have triggered the MSC[4,6], clearly post-date the onset of evaporite deposition by 200–260 kyr and pre-date the isolation event by 100–160 kyr. Therefore, obliquity-controlled, glacio-eustatic lowering of sea level may only have added a minor contribution to the restriction and isolation processes. On the contrary, the onset of the MSC clearly coincides with the amplitude increase in insolation following the ~400-kyr eccentricity minimum dated around 6.0–6.1 Myr, suggesting that long-term orbital cycle forcing superimposed on a directional trend (for example, tectonic closure) plays a critical role in the exact timing of the event. The same may also hold for the onset of the Upper Evaporites (~5.6 Myr ago), as well as for other intra-Messinian events such as the Tortonian/Messinian (T/M) boundary event (~7.2 Myr ago) and the marked change in lithology in the Sorbas basin around 6.7–6.8 Myr ago.

The timing of the changes in plate-tectonic spreading rates (Fig. 2) indicate that tectonic processes indeed contributed to the onset of the MSC, but a direct relation is not obvious. Additional evidence for tectonic activity before the MSC comes from the two pre-Messinian Atlantic gateways. Orogenic uplift had already closed the Betic corridor through Spain in the latest Tortonian/earliest Messinian[7,28], and severely constricted the Rifian corridor through Morocco in the earliest Messinian[29]. The exact timing of closure of the entire Rifian corridor is less certain, because large olistolith complexes cover the youngest marine sediments in the central parts. Mammal exchange between Spain and Morocco—signifying a near-landbridge—had already occurred at least 6.1 Myr ago, 140 kyr before the onset of evaporite deposition[28]. These tectonic processes obviously limited the water exchange between the Mediterranean and the Atlantic during the Messinian, and thus probably heralded the onset of the MSC.

Field evidence, showing that marl/sapropel alternations pass upward via diatomites into evaporite/sapropel alternations, indicates that the sedimentary cyclicity in the Lower (16–17 cycles; refs 8, 25) and Upper (7–8 cycles; ref. 30) Evaporites is controlled by astronomical precession. The total number of sedimentary cycles is in good agreement with the total number of precession peaks,

Table 1 Age control for magnetic reversals

Reversal	Astronomical age (Sorbas basin)	HKLLSZ[3]	CK95[16]	SCHPS[11]	CK92[15]	Constant spreading rate age
C3An.1n (y)	6.04 ± 0.01	5.952	5.894	5.875	5.705	6.01
C3An.1n (o)	6.26 ± 0.02	6.214	6.137	6.122	5.946	6.28
C3An.2n (y)	6.44 ± 0.01	6.356	6.269	6.256	6.078	6.43
C3An.2n (o)	6.71 ± 0.03†	6.677	6.567	6.555	6.376	6.73
Nannofossil event		Age (Site 926)[18]	Depth (m.c.d.) (Hole 853B)	Reversal	Depth (m.c.d.) (Hole 853B)	Interpolated age (nannofossils)
1. LO *Discoaster quinqueramus*		5.537	32.67	C3An.1n (y)	38.45	6.02
2. LCO *Amaurolithus amplificus*		6.020	38.50	C3An.1n (o)	NA	NA
3. X *A. amplificus**, *T. rugosus*		6.798	47.80	C3An.2n (y(	43.60	6.45
4. FO *A. amplificus**		6.840	48.25	C3An.2n (o)	46.50	6.69

Comparison of our astronomical polarity reversal ages with the ages according to recently advanced polarity timescales of Hilgen *et al.*[3], Shackleton *et al.*[11] and Cande and Kent[15,16] (upper Table). Error estimates in our astronomical ages refer to the uncertainty in the exact stratigraphic position of the magnetic polarity reversal with respect to the astronomically dated cycles. † Denotes average of the astronomical ages from Sorbas and Crete[3]. The new astronomical ages are in good to excellent agreement with independently derived ages that result from the most constant spreading rates (see also Fig. 2). Note that only a slight discrepancy exist in the ages of C3An.1n(y). Four correlatable nannofossil bioevents with astronomical age and depth from ODP Site 926 (Atlantic) and 853B (Pacific) are used to interpolate the age of the magnetic reversals from Site 853B (lower table; note that C3An.1n (o) was not recovered). Reversal ages are calculated by exporting astronomical ages of the nannofossil events from ODP Site 926. Ages are in Myr; m.c.d. indicates metres composite depth; X denotes cross-over between *Amaurolithus amplificus* (*including transitional forms) and *Triquetrorhabdulus rugosus*; NA, not available.

whereas there is clearly not enough time for a 40-kyr obliquity control, thus excluding glacio-eustasy. Evaporite deposition occurred during precession maxima (insolation minima), during relatively dry periods when evaporation exceeded precipitation. This allowed the Mediterranean to form a giant brine, when outflow of dense Mediterranean waters into the Atlantic was restricted or obstructed by shallow sills in the western Mediterranean gateways. During precession minima (insolation maxima) and relatively wet periods, high freshwater runoff resulted in deposition of sapropel-like sediments. As the average periodicity for precession in Neogene times is 21.7 kyr, the Lower Evaporite and the Upper Evaporite units have a duration of approximately 370 kyr and 175 kyr, respectively. Tentatively calibrating the evaporite and post-evaporite cycles to the insolation curve leaves only a small 'Messinian gap' (between 5.59 and 5.50 Myr ago), during which the desiccation of the Mediterranean and the accompanying isostatic rebound processes[31] (tectonic tilting and erosion) must have occurred. □

Received 5 November 1998; accepted 10 June 1999.

1. Hsü, K. J., Ryan, W. B. F. & Cita, M. B. Late Miocene desiccation of the Mediterranean. *Nature* **242,** 240–244 (1973).
2. Ryan, W. B. F. *et al. Initial Reports of the Deep Sea Drilling Project* Vol. 13 (US Govt Printing Office, Washington, 1973).
3. Hilgen, F. J. *et al.* Extending the astronomical (polarity) time scale into the Miocene. *Earth Planet. Sci. Lett.* **136,** 495–510 (1995).
4. Clauzon, G., Suc, J.-P., Gautier, F., Berger, A. & Loutre, M.-F. Alternate interpretation of the Messinian salinity crisis: Controversy resolved? *Geology* **24,** 363–366 (1996).
5. Butler, R. W. H., Lickorish, W. H., Grasso, M., Pedley, H. M. & Ramberti, L. Tectonics and sequence stratigraphy in Messinian basins, Sicily: constraints on the initiation and termination of the Mediterranean 'salinity crisis'. *Geol. Soc. Am. Bull* **107,** 425–439 (1995).
6. Hodell, D. A., Benson, R. H., Kent, D. V., Boersma, A. & Rakic-El Bied, K. Magnetostratigraphic, biostratigraphic, and stable isotope stratigraphy of an Upper Miocene drill core from the Salé Briqueterie (northwest Morocco): A high-resolution chronology for the Messinian stage. *Paleoceanography* **9,** 835–855 (1994).
7. Wijermars, R. Neogene tectonics in the Western Mediterranean may have caused the Messinian Salinity Crisis and an associated glacial event. *Tectonophysics* **148,** 211–219 (1988).
8. Vai, G. B. in *Miocene Stratigraphy: An Integrated Approach* (eds Montanari, A., Odin, G. S. & Coccioni, R.) 463–476 (Elsevier Science, Amsterdam, 1997).
9. Decima, A. & Wezel, F. Late Miocene evaporites of the Central Sicilian Basin. *Init. Rep. DSDP* Leg 13, 1234–1240 (1973).
10. Lourens, L. J. *et al.* Evaluation of the Pliocene to early Pleistocene astronomical time scale. *Paleoceanography* **11,** 391–413 (1996).
11. Shackleton, N. J., Crowhurst, S., Hagelberg, T., Pisias, N. G. & Schneider, D. A. A new late Neogene time scale: Application to leg 138 sites. *Proc. ODP Sci. Res.* **138,** 73–101 (1995).
12. Sprovieri, R., Di Stefano, E., Caruso, A. & Bonomo, S. High resolution stratigraphy in the Messinian Tripoli Formation in Sicily. *Paleopelagos* **6,** 415–435 (1996).
13. Sierro, F. J. *et al.* Messinian pre-evaporite sapropels and precession-induced oscillations in western Mediterranean climate. *Mar. Geol.* **153,** 137–146 (1999).
14. Laskar, J., Joutel, F. & Boudin, F. Orbital, precessional, and insolation quantities for the Earth from −20 Myr to +10 Myr. *Astron. Astrophys.* **270,** 522–533 (1993).
15. Cande, S. C. & Kent, D. V. A new geomagnetic polarity time scale for the Late Cretaceous and Cenozoic. *J. Geophys. Res.* **97,** 13917–13951 (1992).
16. Cande, S. C. & Kent, D. V. Revised calibration of the geomagnetic polarity time scale for the Late Cretaceous and Cenozoic. *J. Geophys. Res.* **100,** 6093–6095 (1995).
17. Hooper, P. W. P. & Weaver, P. P. E. Paleoceanographic significance of Late Miocene to early Pliocene planktonic foraminifers at deep sea drilling project site 609. *Init. Rep. DSDP* **94,** 925–934 (1987).
18. Raffi, I., Rio, D., d'Atri, A., Fornaciari, E. & Rocchetti, S. Quantitative distribution patterns and biomagnetostratigraphy of middle and late Miocene calcareous nannofossils from equatorial Indian and Pacific Oceans (Legs 115, 130 and 138). *Proc. ODP Sci. Res.* **138,** 479–503 (1995).
19. Backman, J. & Raffi, I. Calibration of Miocene nannofossil events to orbitally tuned cyclostratigraphies from Ceara Rise. *Proc. ODP. Sci. Res.* **154,** 83–99 (1997).
20. Shackleton, N. J. & Crowhurst, S. Sediment fluxes based on an orbitally tuned time scale 5 Ma to 14 Ma, Site 926. *Proc. ODP. Sci. Res.* **154,** 69–82 (1997).
21. Wilson, D. S. Confirmation of the astronomical calibration of the magnetic polarity timescale from sea-floor spreading rates. *Nature* **364,** 788–790 (1993).
22. Cox, A. & Engebretson, D. C. Change in motion of the Pacific plate at 5 Ma. *Nature* **313,** 472–474 (1985).
23. Wilson, D. S. Confidence intervals for motion and deformation of the Juan de Fuca. *J. Geophys. Res.* **98,** 16053–16071 (1993).
24. Cande, S. C., Raymond, C. A., Stock, J. & Haxby, W. F. Geophysics of the Pittman Fracture Zone and Pacific-Antarctic plate motions during the Cenozoic. *Science* **270,** 947–953 (1995).
25. Dronkert, H. Evaporite models and sedimentology of Messinian and Recent evaporites. *GUA Papers of Geology* Series 1, Vol. 24 (1985).
26. McCulloch, M. T. & De Deckker, P. Sr isotope constraints on the Mediterranean environment at the end of the Messinian salinity crisis. *Nature* **342,** 62–65 (1989).
27. Shackleton, N. J., Hall, M. A. & Plate, D. Pliocene stable isotope stratigraphy of Site 846. *Proc. ODP Sci. Res.* **138,** 337–355 (1995).
28. Garcés, M., Krijgsman, W. & Agustií, J. Chronology of the late Turolian deposits of the Fortuna basin (SE Spain): implications for the Messinian evolution of the eastern Betics. *Earth Planet. Sci. Lett.* **163,** 69–81 (1998).
29. Krijgsman, W. *et al.* Late Neogene evolution of the Taza-Guercif Basin (Rifian Corridor; Morocco) and implications for the Messinian salinity crisis. *Mar. Geol.* **153,** 147–160 (1999).
30. Mascle, G. & Heimann, K. O. Geological observations from Messinian and lower Pliocene outcrops in Sicily. *Mem. Soc. Geol. It.* **16,** 127–140 (1976).
31. Norman, S. E. & Chase, C. G. Uplift of the shores of the western Mediterranean due to Messinian desiccation and flexural isostasy. *Nature* **322,** 450–451 (1983).
32. Grindlay, N. R., Weiland, C. M. & Fox, P. J. *Eos* **76,** F573 (1995).

Acknowledgements. We thank C. G. Langereis, W.-J. Zachariasse and M.-F. Loutre for comments on the manuscript. This work was supported by GOA/NWO, NSF, DGCYT and Fundacion Areces.

Correspondence and requests for materials should be addressed to W.K. (e-mail: krijgsma@geo.uu.nl).

The origin of snake feeding

Michael S. Y. Lee*, Gorden L. Bell Jr† & Michael W. Caldwell‡

* *Department of Zoology, University of Queensland, St Lucia, Brisbane, Queensland 4072, Australia*

† *Museum of Geology, South Dakato School of Mines and Technology, Rapid City, South Dakota 57701, USA*

‡ *Paleobiology, Canadian Museum of Nature, PO Box 3443, Station 'D', Ottawa, Ontario K1P 6P4, Canada*

Snakes are renowned for their ability to engulf extremely large prey, and their highly flexible skulls and extremely wide gape are among the most striking adaptations found in vertebrates[1–5]. However, the evolutionary transition from the relatively inflexible lizard skull to the highly mobile snake skull remains poorly understood, as they appear to be fundamentally different and no obvious intermediate stages have been identified[4,5]. Here we present evidence that mosasaurs—large, extinct marine lizards related to snakes—represent a crucial intermediate stage. Mosasaurs, uniquely among lizards, possessed long, snake-like palatal teeth for holding prey. Also, although they retained the rigid